Investigation of the Hellenistic period pottery production technology from the Seyitömer Mound (Kütahya/Turkey)

C. Serkaya[1], A. İssi[1], V. Uz[1] & A. N. Bilgen[2]
[1]*Department of Materials Science and Engineering, Dumlupınar University, Turkey*
[2]*Department of Archaeology, Dumlupınar University, Turkey*

Abstract

Anatolia has hosted many civilizations from ancient times to the present. There are many settlements belonging to past civilizations. One of them is the Seyitömer Mound. The Seyitömer Mound is located 25 km northwest of Kütahya. It is a 5,000 year-old mound. It has been enlightened that the Seyitömer Mound has been inhibited by civilizations in the Bronze Age, Achaemenid, Hellenistic and Roman periods. From the excavations performed between 2006 and 2013, over 7,000 inventorial and 20,000 finds to be examined have been delivered to the Archaeological Museum of Kütahya and 1,381 artifacts have been exhibited in one of the first private museums belonging to archaeological excavation sites in Turkey at Dumlupınar University. In this study, chemical and mineralogical/phase composition of 30 pottery body sherds unearthed in the Seyitömer Mound belonging to the Hellenistic Period (334–330 BC) have been investigated. Chemical analysis of samples was obtained by wavelength dispersive X-ray fluorescence (WDXRF) and mineralogical/phase composition was obtained by X-ray diffraction (XRD). Scanning electron microscopy (SEM) and microanalysis technique (EDX) were performed for microstructural and microchemical analysis. Thermal analysis (TG–DTA) was also employed as a complementary characterization technique to estimate firing temperature of the potsherds. From the results, ceramic bodies have been produced from clay deposits rich in iron, containing illitic type minerals and carbonated minerals such as calcite and dolomite. Raw materials contain calcite-rich and magnesium minerals. Firing temperatures of the potsherds range from 600°C to 1100°C.
Keywords: Seyitömer Mound, Hellenistic period, ceramic artifact, characterization, archaeometry.

WIT Transactions on The Built Environment, Vol 168, © 2015 WIT Press
www.witpress.com, ISSN 1743-3509 (on-line)
doi:10.2495/SD150541

1 Introduction

Civilizations existed in Anatolia and their belongings became a huge cultural heritage. Every effort like evaluation, conserving or restoration to carry them to future of these artifacts is valuable. Archaeometrical studies gather different branches of science such as materials science, physics, chemistry and others. Archaeological ceramics may be investigated with different characterization techniques to enlighten production technology of the wares (Papachristodoulou *et al.* [1], Barone *et al.* [2]).

The Seyitömer Mound is located 25 km northwest of the centre of Kütahya province. The Mound is 150x140 m in size and has a height of 23.5 m. In order to receive 12 million tonnes of coal reserve under the Mound, archaeological excavations are being held in the archaeological site. The archaeological excavations were started in 1989. It has been enlightened that the Seyitömer Mound has been inhabited by civilizations in the Bronze Age, Achaemenid, Hellenistic and Roman periods (Bilgen [3]). 30 pottery sherds unearthed in the Seyitömer Mound belonging to the Hellenistic period have been investigated. Chemical analysis of samples was performed by wavelength dispersive X-ray fluorescence (WDXRF) and mineralogical/phase composition analysis was performed by X-ray diffraction (XRD) (Vinagre *et al.* [4], Demirel *et al.* [5], Kennett *et al.* [6]) to perform archaeometrical characterization of the artifacts. Scanning electron microscopy (SEM) and energy dispersive spectroscopy (EDS) used for identification of microstructural and microchemical properties of the samples. Thermogravimetric–differential thermal analysis (TG–DTA) was performed to observe the thermal behaviors of the samples to predict the maximum firing temperatures.

Figure 1: A photograph and a map showing the location of the Seyitömer Mound.

2 Materials and methods

The representative photos of the Hellenistic period samples coded as H8, H14, H15 and H20 were given in Figure 2.

Determined parts of the samples were cut by diamond cutting discs and 0.8–1.5 g of samples were obtained. Samples were stored in deionized water to remove impurities for 2 days. Cleaned samples were dried at room temperature. Powder

Figure 2: Photos of H8, H14, H15 and H20 coded samples.

of the samples was prepared in agate mortars to perform the analysis. A Rigaku Miniflex powder diffractometer with Cu Kα radiation (λ=1.5418 Å) was used for the mineralogical analysis. XRD patterns were obtained by scanning 5° to 55° in 2θ, with a goniometer speed of 2°/min, operating at 40 kV and 30 mA. The interpretation of mineralogical content of the data was conducted with JADE 7 software by searching and matching the powder diffraction files. A Rigaku ZSX primus wavelength dispersive X-ray fluorescence (WDXRF) instrument was used for chemical analysis of the elements. The measurements were carried out on glass tablets prepared by fluxing powdered samples with $Li_2B_4O_7$ in 1:10 weigh ratio. The calculation of the semi-quantitative results was conducted with ZSX software. The results were given as oxides. The microstructural and microchemical aspects of the representative potsherds were investigated using FEI Nova Nano 650 SEM instrument. Setaram Labsys Evo instrument was used for TG–DTA analysis. A heating rate of 10°C/min was performed in oxidative atmosphere from room temperature to 1200°C.

3 Results and discussions

3.1 Chemical analysis result and discussion

Instead of giving all the results of the study, chemical analysis results belonging to H8, H14, H15 and H20 which are calcium poor and rich and representing chemical analysis of ceramic groups were given in Table 1.

As seen from the results, the maximum percentage of CaO belongs to H20 coded sample, the minimum percentage belongs to H15 coded sample. Considering total of alkaline and alkaline-earth oxides, H20 has the maximum quantity.

3.2 Mineralogical/phase analysis results and discussion

Determined minerals/phases for the samples are: Quartz (SiO_2), Plagioclase, Illite ($(K,H_3O)Al_2Si_3AlO_{10}(OH)_2$), Microcline ($KAlSi_3O_8$), Calcite ($CaCO_3$), Muscovite ($KAl_2(Si_3Al)O_{10}(OH,F)_2$), Gehlenite ($Ca_2Al_2SiO_7$), Dolomite ($CaMg(CO_3)_2$), Hematite ($Fe_2O_3$), Maghemit ($Fe_20_3$), Blue Dioptase ($CuSiO_2(OH)_2$), Hedenbergite ($CaFe^{+2}SiO_2O_6$). XRD analysis results of H8, H14, H15 and H20 coded samples and raw materials of clays are given in Table 2.

Table 1: Chemical analysis results of H8, H14, H15 and H20. The term of "n.d." indicates not detected or under the limits of detection by WDXRF technique performed.

	Calcium Rich		Calcium Poor	
Oxide	**H8**	**H20**	**H14**	**H15**
Na_2O	1.3622	1.8263	1.7577	3.7479
MgO	4.5568	3.7391	9.2439	3.8566
Al_2O_3	17.7377	11.0083	14.4558	13.8415
SiO_2	54.9392	48.4078	58.7664	66.2611
P_2O_5	0.293	0.3288	0.1303	0.1496
SO_3	0.1149	0.173	0.0577	0.1202
CI	0.0394	0.1273	0.0658	0.2906
K_2O	3.6782	2.4415	2.4104	2.4392
CaO	9.9239	25.8409	1.673	1.0684
TiO_2	0.8235	0.5381	0.6454	0.7514
V_2O_5	n.d.	n.d.	n.d.	n.d.
Cr_2O_3	0.0449	0.0584	0.1815	0.0742
MnO	0.1099	0.1842	0.1661	0.1341
Fe_2O_3	6.2633	5.185	9.9196	7.0957
Co_2O_3	n.d.	n.d.	n.d.	n.d.
NiO	0.0231	0.0406	0.1316	0.058
CuO	0.0157	n.d.	0.015	0.0154
ZnO	0.0288	0.0157	0.0235	0.0194
As_2O_3	n.d.	n.d.	n.d.	n.d.
Rb_2O	n.d.	n.d.	n.d.	0.0367
SrO	0.0235	0.0616	0.0144	0.0124
ZrO_2	0.0219	0.0236	0.0165	0.0277
BaO	n.d.	n.d.	0.3253	n.d.
SnO_2	n.d.	n.d.	n.d.	n.d.
Nb_2O_5	n.d.	n.d.	n.d.	n.d.
Ag_2O	n.d.	n.d.	n.d.	n.d.

Table 2: XRD analysis results of H8, H14, H15 and H20 coded samples and raw materials of clays.

Sample Code	Minerals/Phases
H8	Quartz, Plagioclase, Illite, Microcline, Calcite, Gehlenite, Hematite, Maghemite.
H14	Quartz, Plagioclase, Illite, Microcline, Blue Dioptase, Maghemite.
H15	Quartz, Plagioclase, Muscovite, Gehlenite, Hedenbergite.
H20	Quartz, Plagioclase, Muscovite, Calcite, Dolomite, Maghemite.
SNLKKY	Quartz, Plagioclase, Illite/Muscovite, Montmorillonite, Kaolinite, Calcite, Dolomite.
AYVALIB	Quartz, Plagioclase, Illite/Muscovite, Talc, Kaolinite, Kaliophilite, Calcite, Dolomite.
CKOY2B	Quartz, Plagioclase, Illite/Muscovite, Kaolinite/Montmorillonite, Calcite.
IK3A	Quartz, Plagioclase, Illite/Muscovite, Talc, Montmorillonite, Kaolinite, Calcite.
SO1K	Quartz, Plagioclase, Illite/Muscovite, Montmorillonite, Kaolinite, Calcite, Dolomite.

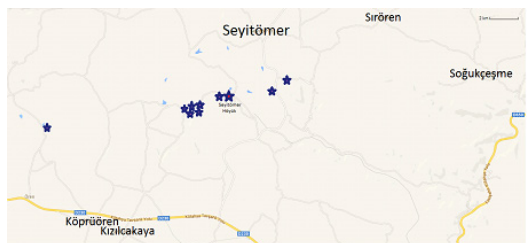

Figure 3: Shows the raw materials (clays) collected around the Seyitömer Mound.

XRD results of the raw materials (clays) collected around the Seyitömer Mound are also given in Table 2. They were coded as SNLKKY, AYVALIB, CKOY2B, IK3A and SO1K.

Quartz is a mineral with high heat of melting. For this reason, quartz mineral exists in all samples. Quartz and feldspars can persist up to 1000°C (İssi *et al.* [7]). Gehlenite begins to form at 800°C and disappear at 900°C (Veniale [8]). Illite/muscovite or mica structure breaks down in the range of 900–1000°C (Grimshaw [9]). Gehlenite may be formed at 850°C with the reaction of CaO and illite structure, diopside may be generated from dolomite and silica reactions at 800–900°C (Cultrone *et al.* [10]).

H14, H15 and H20 coded samples contain illite/muscovite minerals. They could have been fired under 1000°C. H8 coded sample contains gehlenite mineral. H8 coded sample possibly sintered around 800°C. Calcite and dolomite

decomposition begin under 700°C and is completed up to 850°C (López-Arce *et al.* [11]). Therefore, H20 coded sample could have been fired in the lowest temperature. Another suggestion from the results is related with the atmosphere of firing. Hematite indicates oxidative firing (Damjanovic *et al.* [12]). However, existence of maghemite phase on XRD pattern cannot be excluded but, reductive atmosphere should have been provided for firing (Legodi and de Waala [13]). H14 sample contains blue dioptase. Dioptase decomposition begins around 400°C and it is completed at 730°C (Frost and Xi [14]). Therefore, estimated firing temperature could not exceed these firing temperature ranges.

3.3 SEM analysis results and discussion

SEM images of Ca rich and poor samples are given in Figure 4.

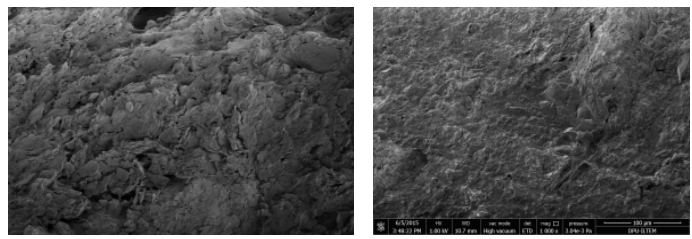

(a) (b)

Figure 4: SEM images of Ca rich H20 coded sample (a) and Ca poor H15 coded sample (b).

Some changes with increasing temperature in clay based ceramics can be described as; interactions between clay matrix and grains, shape changes of grains, increase of the aggregation rate within the clay matrix with the formation of secondary porosity and formation of intergranular bridges. These changes become more evident in calcareous clays than the siliceous materials including clays (Riccardi *et al.* [15]). Since some of the samples contain high amounts of calcium, SEM images exhibited predominantly arrangements of calcium rich new mineral formations in the microstructure of the samples (Figure 4(a)). Quartz is one of the primary components of clay based ceramics with high melting temperature. It is considered that quartz is relatively insoluble below 1250°C, dissolution of quartz forms silica-rich amorphous solution rims around quartz grains (Iqbal and Lee [16]). Quartz grain dissolution into vitrified clay matrix of the sample may easily be distinguished by the atomic contrast difference in BSE images. Feldspar is believed to melt around 1100°C in the contact zone between feldspar crystals and clay relicts and potash matrix require high temperature around 1200°C.

3.4 Thermogravimetric–differential thermal analysis (TG–DTA) results and discussion

Changes occurred due to the decomposition, transformation and formation reactions during a controlled heating process may be examined from TG–DTA

method (Drebushchak *et al.* [17]). Samples were heated from room temperature to 1200°C with a heating rate of 10°C/min in order to expose the enthalpy changes (plotted by DTA curves with endothermic and exothermic effects) and weight loss/gain (plotted by TG curves). The endothermic effect from room temperature to 200°C is due to the release of hygroscopic water (Maritan *et al.* [18]). At higher temperatures of 200–300°C the endothermic effect depicts the removal of the chemically bound water, but it may not met in the present study (Paama *et al.* [19]). Depending on the area of the peaks observed in the range of 200–650°C, the exothermic effect identified within these temperatures was attributed to the combustion of organic materials, not completely burnt during firing in reducing condition and transformed into carbonaceous particles, which are thought to be deliberately added into the ceramic paste to increase its plasticity or were contained in the clay utilized in the manufacture (Palanivel and Rajesh Kumar [20]). The endothermic effects observed at 700–875°C indicated the decarbonation reactions of mainly calcite and dolomite (Meyvel *et al.* [21]).

TG–DTA results of selected samples are given in Figures 5 and 6.

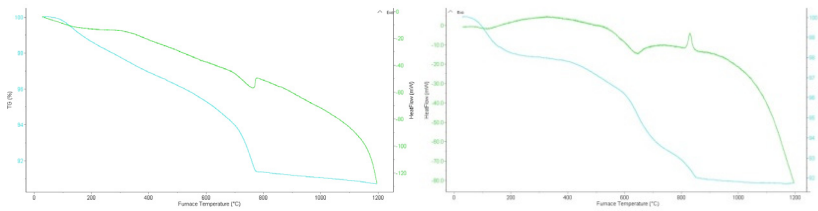

(a) (b)

Figure 5: TG–DTA curve of the sample of H8 (a) and H14 (b).

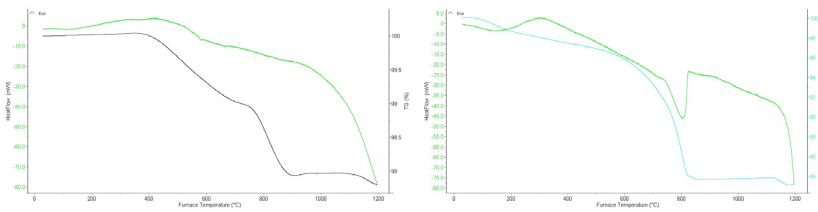

(a) (b)

Figure 6: TG–DTA curve of the sample of H15 (a) and H20 (b).

As it can be seen from Figure 5, mass loss peak in H8 coded sample is 8%. Mass change is methodical up to 680°C. Considering TG analysis with XRD results weight originates from that heats are from the reactions of unbound or adsorbed water loss or burning of organic substance. According to DTA analysis endothermic reactions in 770°C depends on calcite decomposition for H8 coded sample. Mass loss peak in H14 coded sample is around 8% and similar with H8 coded sample. DTA analysis shows the endothermic reaction in 640°C depends

on calcite decomposition for H14 coded sample. Also exothermic reaction in 840°C shows new crystallizations are occurred. Mass loss peak in H15 coded sample is around 2.5%. DTA analysis shows the endothermic reaction in 575°C depends on crystal water decomposition for H15 coded sample. Mass loss peak is around 15% in H20 coded sample and exothermic reaction in 300°C occurred organic based component burnt. Endothermic reaction in 800°C depends on calcite decomposition for H20 coded sample.

4 Conclusions

From WDXRF, XRD, SEM and TG–DTA analysis results obtained, the Hellenistic period ceramics unearthed in the Seyitömer Mound have been produced from clay deposits containing illitic type minerals with rich in iron and calcium rich and poor accessory minerals. To compare with regional geological formations and raw material sources, it may be suggested that local raw material source is enough to produce such kind of ceramic wares during the Hellenistic period. According to phases/minerals in Hellenistic period samples firing temperatures are between 600°C and 1100°C.

Acknowledgement

This study is a part of ongoing project titled “Archaeometrical Characterization of Ceramic Findings Belonging to Achaemenid, Hellenistic and Roman Periods from Seyitömer Mound (Kütahya)” with the project number of 113K096. The Scientific and Technological Research Council of Turkey (TÜBİTAK) is acknowledged.

References

[1] Papachristodoulou C., Oikonomou A., Ioaniddes K. & Gravani K., A Study of Ancient Pottery by Means of X-Ray Fluorescence Spectroscopy, Multivariate Statistics and Mineralogical Analysis. Analytica Chimica Acta., 573, pp. 347-353, 2006.

[2] Barone G., Crupi V., Galli S., Majolino D., Migliardo P. & Venuti V., Spectroscopic İnvestigation of Greek Ceramic Artefacts. Journal of Molecular Structure, 651, pp. 449-458, 2003.

[3] Bilgen, A.N., Seyitömer Höyük Kazısı Ön Raporu. P.1 Kütahya, 2011 (in Turkish).

[4] Vinagre U. M., Latini R. M., Bellido A. V. B., Buarque A. & Borges A. M., Ancient Ceramics Analysis by Neutron Activation in Association with Multivare Methods, Brazilian Journal of Physics, 35, pp. 779-781, 2005.

[5] Demirel M., Sevin F. B., Say R. & Yazan Y., Propranolol HCl Imprinted Polymeric Microspheres: Development, Characterization and Dissolution. FABAD J. Pharm. Sci., 32, pp. 147-157, Ankara, 2007.

[6] Kennett D. J., Sakai S., Neff H., Gossett R. & Larson D. O., Compositional Characterisation of Prehistoric Ceramics: A New Approach. Journal of Archaeological Science, 29, pp. 443-455, 2002.
[7] Issi, A., Kara A. & Alp, A.O., An Investigation of Hellenistic Period Pottery Production Technology from Harabezikan/Turkey. Ceramics International, 37, pp. 2575-2582, Eskişehir, 2011.
[8] Veniale F., Modern techniques of analysis applied to ancient ceramics. In: Advanced workshop on analytical methodologies for the investigation of damaged Stones, Pavia, (Italy), 1990.
[9] Grimshaw R.W., The Chemistry and Physics of Clays. Techbooks, p. 727, India, 1971.
[10] Cultrone G., Navarro C. R., Sebastian E., Cazalla O. & Torre M. J., Carbonate and Silicate Phase Reactions during Ceramic Firing. Eur. J. Mineral, 13, pp. 621-634, Stuttgart (Germany), 2001.
[11] López-Arce P., Garcia-Guinea J., Gracia M. & Obis J., Bricks in historical buildings of Toledo City: characterisation and restoration. Mater. Charact., 50, pp. 59-68, 2003.
[12] Damjanovic L., Antunovic I. H., Mioc U. B, Bikic V., Milanovic D. & Evans I. R., Archaeometric study of medieval pottery excavated at Stari (Old) Ras Serbia. J. Archaeol. Sci., 38, pp. 818-828, 2011.
[13] Legodi, M. A. & de Waala M. A. The preparation of magnetite, goethite, hematite and maghemite of pigment quality from mill scale iron waste. Department of Chemistry, University of Pretoria, v.74, i.1, pp. 161-168, Pretoria (South Africa), 2007.
[14] Frost L. R. & Xi Y. Thermogravimetric analysis of the copper silicate mineral dioptase. Journal of Thermal Analysis & Calorimetry. Vol. 112, Issue 2, pp. 615-619, 2013.
[15] Riccardi M. P., Messiga B. & Duminuco P., An approach to the dynamics of clay firing. Appl. Clay Sci., 15, pp. 393-409, 1999.
[16] Iqbal Y. & Lee W. E., Microstructural evolution in triaxial porcelain. J. Am. Ceram. Soc., 83, pp. 3121-3127, 2000.
[17] Drebushchak V. A., Mylnikova L. N., Drebushchak T. N. & Boldyrev V. V., The investigations of ancient pottery. J. Therm. Anal. Calorim., 82, pp. 617-626, 2005.
[18] Maritan L., Nodari L., Mazzoli C., Milano A. & Russo U., Influence of firing conditions on ceramic products: experimental study on clay rich in organic matter. Appl. Clay Sci., pp. 311-315, 2006.
[19] Paama L., Pitkanen I. & Peramaki P., Analysis of archaeological samples and local clays using ICP-AES, TGDTG and FTIR techniques. Talanta, 51, pp. 349-357, 2000.
[20] Palanivel R. & Rajesh Kumar U., Thermal and spectroscopic analysis of ancient potteries. Rom. J. Phys., 56, pp. 195-208, 2011.
[21] Meyvel S., Sathya P. & Velraj G., Thermal characterization of archaeological potsherds recently excavated in Nedunkur, Tamilnadu, India. Cerâmica, 58, pp. 338-341, 2012.